

# The Crystal Structure of Fluoride-inhibited Cytochrome *c* Peroxidase\*

(Received for publication, March 26, 1984)

Steven L. Edwards‡, Thomas L. Poulos§, and Joseph Kraut

From the Department of Chemistry, University of California, San Diego, La Jolla, California 92093

The three-dimensional crystal structure of yeast cytochrome *c* peroxidase complexed with fluoride ( $F^-$  or HF) has been determined by difference Fourier techniques and partially refined at 2.5-Å resolution. Fluoride binding induces significant perturbations of the enzyme structure of the distal side of the heme. The major effect occurs at the active-site arginine residue (Arg-48) which moves about 2 Å in order to optimize hydrogen-bonded interactions with the fluorine atom. A small readjustment of the distal histidine (His-52), about 0.5 Å, is also seen upon fluoride binding. Additionally, a hydrogen-bonded network of 4 water molecules at the active site is reorganized. No significant movements are detectable in either the heme itself or in the proximal histidine ligand. These observations imply that movement of the Arg-48 side chain may play a key role in the enzymic mechanism of cytochrome *c* peroxidase.

Although we cannot unequivocally determine whether fluoride is bound as HF or  $F^-$ , the hydrogen-bonding pattern around the ligand points to the protonated form. Structural comparison suggests that there is a difference between the tautomeric state of the imidazole side chain of the distal histidine in cytochrome *c* peroxidase and of the similarly positioned distal histidine in the globins. This difference accounts for the observation that cytochrome *c* peroxidase preferentially binds the protonated form of ligands, whereas the globins bind the anionic form. The tautomer indicated by the peroxidase structure is the one required for acid base catalysis (Poulos, T. L., and Finzel, B. C. (1984) in *Peptide and Protein Reviews* (Decker, M., ed) in press).

Yeast cytochrome *c* peroxidase is a monomeric heme enzyme ( $M_r = 34,000$ ) found in yeast mitochondria, where it catalyzes the reaction shown below and operates as a possible alternative terminal oxidase in respiration (Erecinska *et al.*, 1973).



Cytochrome *c* peroxidase is perhaps the most thoroughly characterized of the heme enzymes (Yonetani, 1976); it is the only one for which a high-resolution crystallographic analysis

\* The work was supported by Grant PCM 82-08414 from the National Science Foundation and by Grants RR 00757 and GM 01928 from the National Institutes of Health. This paper is based in large part on experiments and preliminary analysis presented in the Ph.D dissertation of S. L. E. The costs of publication of this article were defrayed in part by the payment of page charges. This article must therefore be hereby marked "advertisement" in accordance with 18 U.S.C. Section 1734 solely to indicate this fact.

‡ To whom reprint requests should be sent.

§ Present address, Genex Corp., Science and Technology Center, 16020 Industrial Drive, Gaithersburg, MD 20877.

has been carried out (Poulos *et al.*, 1980; Finzel *et al.*, 1984). Based on the wealth of structural and biochemical information available for cytochrome *c* peroxidase and other peroxidases, stereochemical models have been proposed for the reaction between the enzyme and peroxides which produce cytochrome *c* peroxidase Compound I (often called the ES complex) and for the subsequent reduction of Compound I by ferrocyanochrome *c* (Poulos and Kraut, 1980a and 1980b). Of fundamental importance in these proposals are the acid base catalytic role of the distal histidine, His-52, and charge stabilization by Arg-48, both of which are invariant in all plant peroxidases for which sequence information is available (Welinder, 1976; Welinder and Mazza, 1977; Takio *et al.*, 1980). Arg-48 also participates in a hydrogen-bonding network that connects the interior distal side of the heme with the enzyme surface (Finzel *et al.*, 1984), and we have postulated that this network provides a conduit for the transfer of protons and electrons (Poulos and Kraut, 1980a; Edwards, 1981; Poulos and Finzel, 1984).

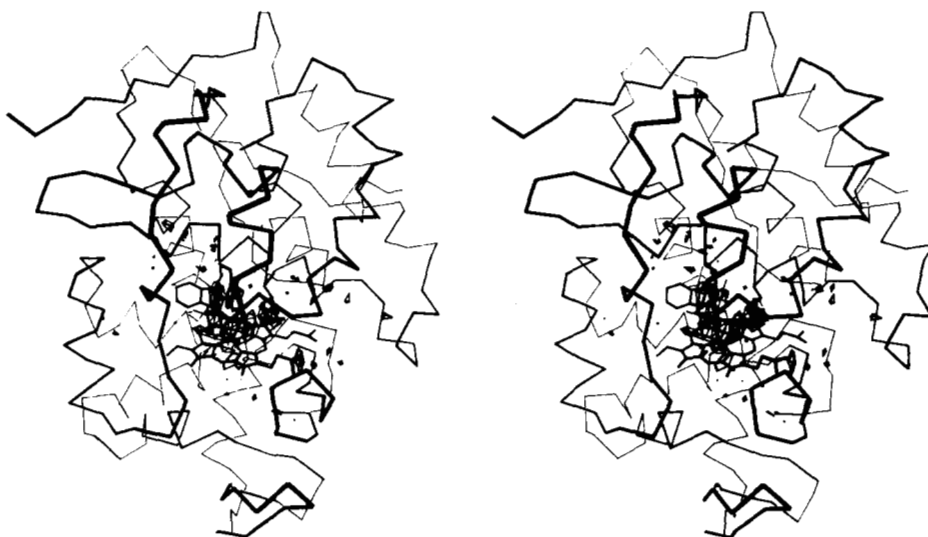
In order to test these hypotheses, one would like to trap the crystalline cytochrome *c* peroxidase- $\text{H}_2\text{O}_2$  complex or crystallize the cytochrome *c* peroxidase-cytochrome *c* complex and determine precisely how the cytochrome *c* molecule interacts with substrate molecules. Unfortunately, the reaction between cytochrome *c* peroxidase and  $\text{H}_2\text{O}_2$  is so fast that trapping the enzyme substrate complex would be extremely difficult, and crystallization conditions for the cytochrome *c* peroxidase-cytochrome *c* complex have continued to elude us. Instead, we have studied the binding of various ligands to cytochrome *c* peroxidase to determine how the enzyme structure responds to steric and electronic perturbations at the peroxide binding site. Although such experiments yield only indirect evidence relevant to the catalytic mechanism, they are capable of furnishing insights into possible dynamics at the active site. Moreover, the availability of a highly refined structure for native cytochrome *c* peroxidase (Finzel *et al.*, 1984), together with further refinement of the fluoride complex now permits a much more precise determination than was previously possible of how small-molecule ligands affect the enzyme's structure. Here we report the effect of fluoride on the structure of cytochrome *c* peroxidase, a high-spin complex.

## MATERIALS AND METHODS

Cytochrome *c* peroxidase was purified and crystallized as previously described (Poulos *et al.*, 1978). The fluoride complex was formed by soaking cytochrome *c* peroxidase crystals in an artificial mother liquor consisting of 30% 2-methyl-2,4-pentanediol, 0.05 M potassium phosphate, pH 6.0, and 1 mM sodium fluoride. Conversion of the crystals to the fluoride form was easily monitored by visual inspection since the fluoride complex appears green under fluorescent light while parent crystals are brownish-red (under incandescent white light both forms appear red). The visible absorption spectrum of the dissolved fluoride-soaked crystal was recorded after data collection and the crystal was judged to be at least 80% in the fluoride form.

A single crystal was used for collection of a complete data set to 2.5-Å resolution using the locally developed multiwire area detector

FIG. 1. The  $(F_{\text{fluoride}} - F_{\text{parent}})\alpha_{\text{parent}}$  difference Fourier map superimposed on an  $\alpha$  carbon backbone model of cytochrome *c* peroxidase. Also shown are key active-site residues: Arg-48, Trp-51, His-52, and His-175.



diffractometer (Cork *et al.*, 1975). Data were collected at 40 s/frame with steps of  $0.06^\circ$  between frames. A total of 60,613 observations of 19,539 independent reflections were measured to give a complete octant of data in space group  $P2_12_12_1$  to 2.5 Å. At the end of data collection the decay in initial intensities was about 13.8%.

All Bijvoet-pair data were merged to give a single structure factor and the final overall scaling residual,  $R_{\text{sym}}$ ,<sup>1</sup> was 6.5%. With the exception of crystallographic refinement, all subsequent data manipulations were carried out with the XTAL system of computer programs (Hall *et al.*, 1980).

Phases used for initial Fourier syntheses were based on the refined ( $R = 0.21$ ) 1.7-Å structure of native cytochrome *c* peroxidase (Finzel *et al.*, 1984). Details of that refinement will be presented elsewhere.

Initially, an  $F_{\text{fluoride}} - F_{\text{parent}}$  difference Fourier using refined parent phases ( $\alpha_{\text{parent}}$ ) was examined. Those side chains and solvent molecules which the difference Fourier showed had moved in response to fluoride binding were deleted from the cytochrome *c* peroxidase model and two cycles of restrained least-squares refinement (Hendrickson and Konert, 1980) using the fluoride data were carried out. An  $(F_{\text{c}} - F_{\text{c}})_{\text{fluoride}}$  difference Fourier using refined fluoride phases ( $\alpha_{\text{fluoride}}$ ) was then used to accurately position those residues and solvent molecules which had been perturbed.

The background level for all electron density difference maps was taken as  $\sigma =$  the root mean square difference density over an entire asymmetric unit. The minimum contour level considered significant was at  $\pm 3\sigma$ .

Model building and interpretation of electron density difference maps was carried out with the aid of an Evans and Sutherland Picture System.

## RESULTS

**Fluoride-Parent Difference Fourier**—Fig. 1 shows the  $(F_{\text{fluoride}} - F_{\text{parent}})\alpha_{\text{parent}}$  difference electron density map superimposed on the entire cytochrome *c* peroxidase model and demonstrates that all significant changes are confined to the active site. Fig. 2 is a more detailed view of the active-site region. In addition to key active-site residues, all ordered water molecules in the active site that were found during the course of refinement are shown.

The most dramatic and clearly defined change is in the location of Arg-48. A  $7\sigma$  envelope of negative density surrounds the Arg-48 side chain and is flanked by a corresponding  $7\sigma$  envelope of positive density, clearly demonstrating that Arg-48 moves about 2 Å in response to fluoride binding. The

direction of movement is away from the heme propionates and toward the distal side axial heme coordination position where Arg-48 forms a hydrogen bond with the fluorine atom. This movement results in the expulsion of the bound solvent molecule, water 648.

His-52 is also perturbed as evidenced by  $\pm 3\sigma$  lobes of difference density bracketing the imidazole ring, although precisely how the His-52 side chain should be repositioned is not immediately evident from the difference map alone. A more quantitative assessment of this movement was obtained by subsequent crystallographic refinement (see below).

A  $7\sigma$  positive density peak near the distal-side axial coordination position is undoubtedly due to the bound fluorine atom, although its precise location is complicated by perturbations of surrounding water molecules. Additionally, the difference map must be interpreted with caution in this region since simply replacing the axial water ligand (water 595, Fig. 2) with a fluoride ion would result in no net change in the number of electrons at this site.

The appearance of any difference density at all indicates that the fluoride has either a higher occupancy, a different temperature factor, or is bound in a slightly different position than the water ligand in the native structure. Unfortunately at 2.5-Å resolution we cannot determine the relative contribution of each of these possibilities. However, the size, shape, and position of the density leads us to believe that the fluoride ligand is bound with higher occupancy than the native water, which is judged to be about 70% occupied, and that in the native structure the water may be slightly displaced from the heme axis in the direction of Arg-48 whereas the fluoride is probably right on the axis.

Finally, a small lobe of negative difference density is situated between the proximal heme ligand (His-175) and the iron atom, although we cannot detect any movement of either the heme or of His-175. We surmise that this feature indicates a decrease in electron density between His-175 and the iron atom, perhaps due to weakening of the N-Fe bond or to a slight increase in the N-Fe bond length. We cannot be more specific about this feature without extending the data to higher resolution.

**Crystallographic Refinement**—While the difference Fourier map just described offers a semiquantitative estimate of fluoride-induced conformation changes, precise repositioning of those atoms that are perturbed, with the possible exception of Arg-48, cannot be made with confidence from the map

$$^1 R_{\text{sym}} = \sum_{hkl} \frac{\sum_i |I_i - \langle I \rangle|}{\sum_i I_i}$$

where  $I_i$  is the observed intensity of  $i$ th reflection and  $\langle I \rangle$  is the scaled mean intensity.

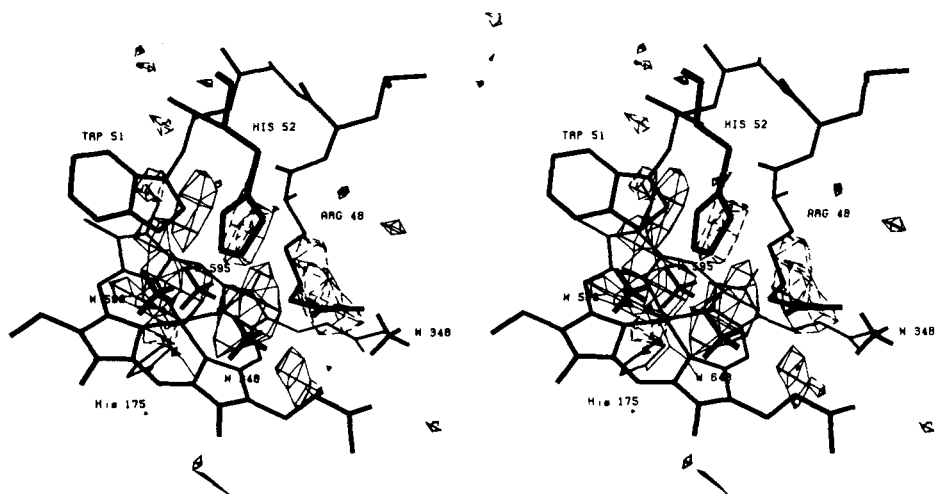


FIG. 2. A close-up view of the  $(F_{\text{fluoride}} - F_{\text{parent}})_{\alpha_{\text{parent}}}$  difference Fourier map superimposed on the native cytochrome *c* peroxidase active site. The minimum contour level is  $\pm 3\sigma$ .

FIG. 3. The  $(F_o - F_c)_{\text{fluoride} \alpha_{\text{fluoride}}}$  difference Fourier map. Arg-48, His-52, the fluorine atom, and water NW were manually fitted to the difference map. The fluorine atom is represented by a tetrahedral shape for plotting convenience. The minimum contour level is  $\pm 5\sigma$ .

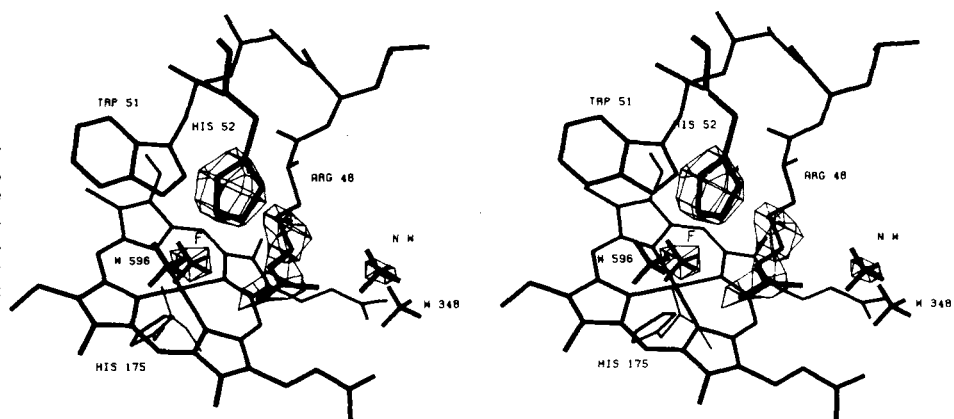
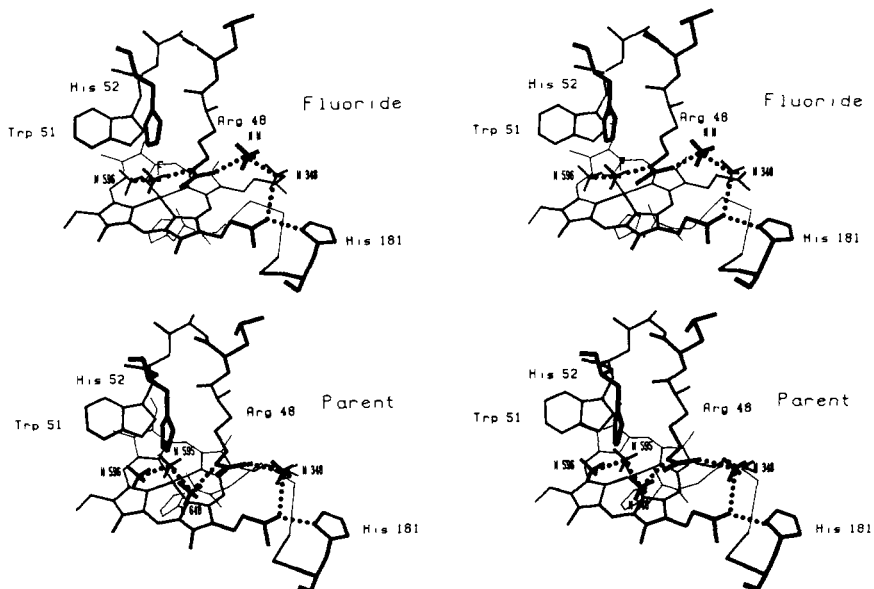


FIG. 4. The cytochrome *c* peroxidase active site structure after (upper) and before (lower) fluoride binding.



alone. Therefore the fluoride-cytochrome *c* peroxidase complex structure was further refined against x-ray data from the complex using the Konnert-Hendrickson restrained least-squares package of programs (Hendrickson and Konnert, 1980). To determine as accurately as possible the locations of side chains and solvent molecules that were known to have moved from inspection of the difference map, the perturbed

atoms were initially excluded from two cycles of structure factor calculations. Atoms which were removed included the side chains of Arg-48 and His-52 and water molecules 595 and 648. As a result, an  $(F_o - F_c)_{\text{fluoride} \alpha_{\text{fluoride}}}$  difference Fourier map will show the new location of those atoms. Because the number of atoms removed is small relative to the total number included, their overall effect on shifts in atomic positions

during the course of refinement is negligible.

After two cycles of refinement, the *R* factor dropped from 0.22 to 0.18, resulting in a root mean square shift in atomic positions of  $\pm 0.19$  Å. At 2.5-Å resolution, we do not consider a 0.19-Å shift significant, indicating that the fluoride and parent structures are identical within our present limits of accuracy except for those few atoms which move in response to fluoride binding.

*F<sub>o</sub>-F<sub>c</sub> Difference Fourier Map*—Fig. 3 shows the resulting *F<sub>o</sub>-F<sub>c</sub>* difference Fourier map superimposed on the refined fluoride structure. Also shown is the fit of Arg-48, His-52, and the fluorine atom, all of which are considerably more well defined than in the fluoride-parent difference map. Two additional changes are the expulsion of water 648 and acquisition of a new water molecule labeled NW.

*Comparison of the Fluoride and Parent Structures*—Fig. 4 is a comparison of the fluoride-complex and parent active-site structures. The F-Fe bond distance is 2.0 Å, which is 0.4 Å shorter than the water 595 to Fe bond in the parent structure. As a result, His-52 must form a longer hydrogen bond with the hydrogen fluoride than it does with water 595 in the parent structure. In fact, a small displacement of about 0.5 Å in the position of His-52 probably results from its attempt to optimize hydrogen-bonding interactions with the hydrogen fluoride and a second active-site water, water 596.

In the parent structure, Arg-48 does not directly hydrogen-bond with water 595 but instead hydrogen-bonds with water 648 (Fig. 4). When fluoride binds, Arg-48 swings in, displaces water 648 and forms a direct hydrogen bond with the fluorine atom.

One final change to be noted is the acquisition in the active site of a new water molecule (NW, Fig. 4) which now occupies the position formerly taken by the guanidinium group of Arg-48 in the parent structure. Remembering the movement of Arg-48 expels water 648, comparison of the fluoride and parent structures in Fig. 4 will show that while the location of distal-side residues and the hydrogen-bonding pattern between these residues and ordered water molecules has changed, the total number of active site waters and total number of hydrogen bonds remains unchanged.

## DISCUSSION

*Movement of Arg-48*—The large movement of the Arg-48 side chain in response to fluoride binding is relevant to the proposed role of Arg-48 in both the formation of Compound I (Poulos and Kraut, 1980a; Poulos, 1982) and electron transfer from ferrocyanochrome *c* (Poulos and Kraut, 1980b; Poulos and Finzel, 1984). Heterolysis of the RO-OH bond results in species resembling RO<sup>-</sup> and <sup>+</sup>OH in the activated complex and the suggested role of Arg-48 is to stabilize the developing negative charge on RO<sup>-</sup>, thereby assisting in polarization of the RO-OH bond. Since the present investigation demonstrates that Arg-48 can undergo a considerable repositioning in order to optimize its interaction with a fluorine atom, we can expect similar changes to occur in response to substrate binding in order to optimize stabilization of the activated complex.

The movement of a polar group in response to ligand binding in a globin-like molecule has been observed before. In the structure of cyanide-inhibited erythrocyruorin (Steigeman and Weber, 1979) the distal histidine side chain, E7, which extends toward the surface in the native form, swings inward to make a polar contact with the heme-bound ligand.

More intriguing is the proposed role of Arg-48 in the electron transfer reaction. Fig. 4 illustrates the entire hydrogen-bonding network which extends from water 595 (parent struc-

ture in Fig. 4) in the active site to His-181 on the enzyme surface. Note that Arg-48 provides a key link between the active site and the molecular surface. Because the cytochrome *c* peroxidase-cytochrome *c* intermolecular interface is postulated to be centered near His-181, the Arg-48 hydrogen-bonding network has been implicated in the transfer of electrons and protons into the cytochrome *c* peroxidase active site (Poulos and Kraut, 1980b; Edwards, 1981).

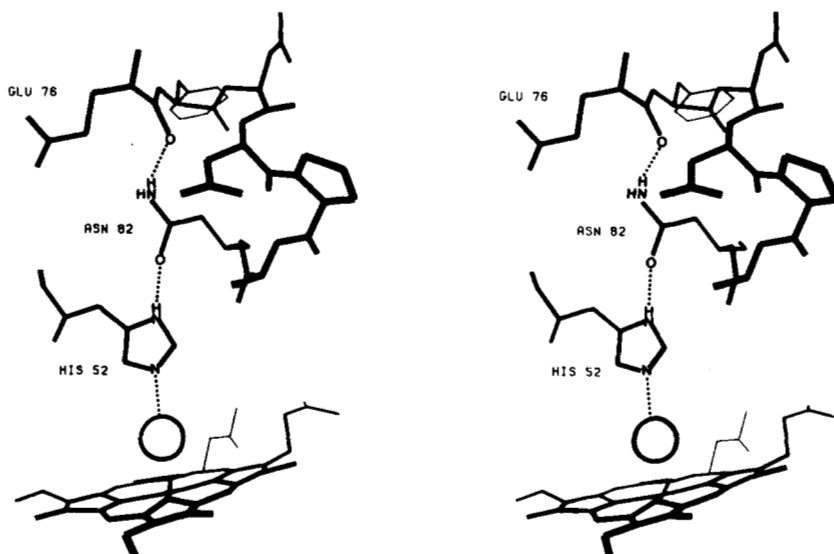
While the actual path of electrons into the active site is a matter for speculation, the proton path may be straightforward. In the native structure at neutral pH, Arg-48 is hydrogen-bonded to water 348 near the protein surface and presumably protonated. The stoichiometry of the reaction, in which two electrons are transferred from two molecules of reduced cytochrome *c* to Compound I, requires that two protons also be supplied to balance charges. It appears that the required proton transfers could be mediated by the side chain of Arg-48 swinging in to hydrogen-bond with the active-site ligand, establishing a solvent structure resembling that shown in Fig. 4 for the fluoride complex (Edwards, 1981). After releasing a proton, the side-chain could swing back away from the active site toward the solvent to be reprotonated.

*Preference for Binding of HF over F<sup>-</sup>*—A long-standing question in heme-protein biochemistry is why peroxidases prefer to bind ligands in the acidic form, HX, rather than as anions, X<sup>-</sup> (Dunford and Alberty, 1967; Ellis and Dunford, 1968; Jones and Middlemiss, 1972; Erman, 1974a, 1974b; Davies *et al.*, 1976; Job and Jones, 1978) while globins will bind anions (Williams, 1974). For example, Erman (1974a, 1974b) has demonstrated that the rate of association of cytochrome *c* peroxidase with HCN, HF, and H<sub>2</sub>O<sub>2</sub> is much faster than with the corresponding anions. Jones and co-workers (Davies *et al.*, 1976) have postulated that peroxidases have negatively charged residues near the active-site entrance which operate as an electrostatic gate to prevent the binding of anions. Examination of the refined cytochrome *c* peroxidase structure reveals that the opening to the ligand access channel, which provides the main entry point to the active site, does contain an aspartate residue but that this aspartate is neutralized by a nearby lysine residue (Finzel *et al.*, 1984). Therefore, anions should not be prevented from entering the access channel and, on the contrary, the presence of Arg-48 at the bottom of the channel should provide an electrostatic attractant for anions.

As an alternative, Poulos and Finzel (1984) have postulated that this preference for HX is due primarily to the hydrogen-bonding interaction which is possible between the distal histidine, His-52, and protonated ligands. Fig. 5 illustrates the hydrogen-bonding network involving His-52. N $\delta$ 1 hydrogen bonds with the side chain carbonyl oxygen atom of Asn-82 and must, therefore, act as a hydrogen-bond donor, leaving N $\epsilon$ 2 unprotonated and able only to act as a hydrogen-bond acceptor. As a result, ligands which are capable of donating hydrogen bonds, HX but not X<sup>-</sup>, will form the more stable complex. In the globins, on the other hand, N $\delta$ 1 is exposed to the solvent (Takano, 1977) and can either accept or donate hydrogen bonds, so that in the case of the globins there is expected to be no preference for HX over X<sup>-</sup> due to this interaction.

The postulated catalytic role of distal His-52 is also consistent with the foregoing tautomeric assignment. In order to act as an acid base catalyst in the transfer of a proton during heterolytic cleavage of H<sub>2</sub>O<sub>2</sub>, the N $\epsilon$ 2 of His-52 must carry an unshared electron pair. Thus the hydrogen atom of the neutral imidazole ring must be located at N $\delta$ 1, where it participates

FIG. 5. Hydrogen-bonding interactions involving the distal histidine, His-52. The carbonyl oxygen atom of Glu-76 hydrogen-bonds with the side chain amido nitrogen atom of Asn-82 leaving the Asn-82 side chain carbonyl oxygen atom to serve as a hydrogen-bond acceptor for N $\delta$ 1 of His-52. As a result, N $\epsilon$ 2 of His-52 can only accept, not donate hydrogen bonds. A generalized ligand at the sixth coordination site is represented by the circle.



in the observed hydrogen bond to the side chain of Asn-82 (Poulos and Finzel, 1984).

Finally, we consider the pH dependence of HF binding. Erman has shown that the interaction of HF, HCN, and H<sub>2</sub>O<sub>2</sub> depends on the deprotonation of a group on the enzyme with a pK = 5.5 (Erman, 1974a and 1974b). One obvious choice for this group is His-52. However, as we have argued elsewhere (Poulos and Finzel, 1984), the pK = 5.5 group could also be the carboxyl group of Asp-235. The side chain of Asp-235 is buried in the internal "proximal pocket" where it hydrogen-bonds with the proximal histidine ligand (Finzel *et al.*, 1984). Hydrogen-bonding interactions with the proximal ligand are considered to play an important role in heme reactivity (Valentine, *et al.*, 1979; Peisach, 1975) and a weakening of the Asp-His hydrogen bond in cytochrome *c* peroxidase by protonation of Asp-235 should have significant effects on ligand-binding properties. However, a pK = 5.5 is not normally expected for either an aspartate or histidine. Nevertheless, we prefer Asp-235 as the pK = 5.5 group because this residue is buried and should have an elevated pK. On the other hand, His-52 is available to solvent molecules via the ligand access channel and we see no compelling reason based on the x-ray structure why His-52 should exhibit a lower pK than expected.

#### REFERENCES

- Cork, C., Hamlin, R. C., Vernon, W., Xuong, N.-H., and Perez-Mendez, V. (1975) *Acta Crystallogr. Sect. A Cryst. Phys. Diffr. Theor. Gen. Crystallogr.* **31**, 702-703
- Davies, D. M., Jones, P., and Mantle, D. (1976) *Biochem. J.* **157**, 247-253
- Dunford, H. B., and Alberty, R. A. (1967) *Biochemistry* **6**, 447-451
- Edwards, S. L. (1981) Ph.D. dissertation, University of California
- Ellis, W. D., and Dunford, H. B. (1968) *Biochemistry* **7**, 2054-2062
- Erecinska, M., Oshino, N., Loh, P., and Brocklehurst, E. (1973) *Biochim. Biophys. Acta* **292**, 1-12
- Erman, J. E. (1974a) *Biochemistry* **13**, 34-38
- Erman, J. E. (1974b) *Biochemistry* **13**, 39-44
- Finzel, B. C., Poulos, T. L., and Krant, J. (1984) *J. Biol. Chem.* **259**, 13027-13036
- Hall, S. R., Stewart, J. M., and Munn, R. J. (1980) *Acta Crystallogr. Sect. A Cryst. Phys. Diffr. Theor. Gen. Crystallogr.* **36**, 979-989
- Hendrickson, W. A., and Konnert, J. H. (1980) in *Computing in Crystallography* (Diamond, R., Ramseshan, S., and Venkatesan, K., eds) pp. 13.1-13.23, Indian Institute of Science, Bangalore, India
- Job, D., and Jones, P. (1978) *Eur. J. Biochem.* **86**, 565-572
- Jones, P., and Middlemiss, D. N. (1972) *Biochem. J.* **130**, 411-415
- Peisach, J. (1975) *Ann. N. Y. Acad. Sci.* **244**, 187-203
- Poulos, T. L. (1982) in *Molecular Structure and Biological Activity* (Griffin, J. E., and Duax, W. L., eds) pp. 79-90, Elsevier Scientific Publishing Co., Amsterdam
- Poulos, T. L., and Finzel, B. C. (1984) in *Peptide and Protein Reviews* (Decker, M., ed) in press
- Poulos, T. L., and Kraut, J. (1980a) *J. Biol. Chem.* **255**, 8199-8205
- Poulos, T. L., and Kraut, J. (1980b) *J. Biol. Chem.* **255**, 10322-10330
- Poulos, T. L., Freer, S. T., Alden, R. A., Xuong, N., Edwards, S. L., Hamlin, R. C., and Kraut, J. (1978) *J. Biol. Chem.* **253**, 3730-3735
- Poulos, T. L., Freer, S. T., Alden, R. A., Edwards, S. L., Skogland, U., Takio, K., Eriksson, B., Xuong, N., Yonetani, T., and Kraut, J. (1980) *J. Biol. Chem.* **255**, 575-580
- Steigeman, W., and Weber, E. (1979) *J. Mol. Biol.* **127**, 309-338
- Takano, T. (1977) *J. Mol. Biol.* **110**, 537-568
- Takio, K., Titani, K., Ericsson, L. H., and Yonetani, T. (1980) *Arch. Biochem. Biophys.* **203**, 615-619
- Valentine, J. S., Sheridan, R. P., Allen, L. C., and Kahn, P. C. (1979) *Proc. Natl. Acad. Sci. U. S. A.* **76**, 1009-1013
- Welinder, K. G. (1976) *FEBS Lett.* **72**, 19-23
- Welinder, K. G., and Mazza, G. (1977) *Eur. J. Biochem.* **73**, 353-358
- Williams, R. J. P. (1974) in *Iron in Biochemistry and Medicine* (Jacobs, A., Worwood, M., eds) pp. 183-219, Academic Press, New York
- Yonetani, T. (1976) *Enzymes* **13**, 345-361